Available online at www.sciencedirect.com
ScienceDirect
Journal of Power Sources 174 (2007) 1063–1068
JOURNAL OF POWER SOURCES
www.elsevier.com/locate/jpowsour

Short communication

Improvement of rate capability in rechargeable lithium-ion batteries using oxide-based active materials–carbon composite cathodes

Tomonari Takeuchi *, Mitsuharu Tabuchi, Kazuaki Ado, Kuniaki Tatsumi

National Institute of Advanced Industrial Science and Technology (AIST), Midorigaoka 1-8-31, Ikeda, Osaka 563-8577, Japan

Available online 30 June 2007

Abstract

$LiNi_{0.8}Co_{0.15}Al_{0.05}O_2$–carbon composite positive electrodes were prepared by the spark-plasma-sintering (SPS) treatment. The SPS treated acetylene black (AB) powder (HDAB) was used as carbon sources, and it showed an effect to improve the electrical connections between the carbon particles. By the SPS treatment of the $LiNi_{0.8}Co_{0.15}Al_{0.05}O_2$ + HDAB blended powder, the strong bindings between the active materials and the carbon powders were formed. Both contact effects, particularly the active material–carbon contact effect, improved the electrochemical performances of the cells. The improvement effects were more evident when the cells were cycled at higher current density, which indicates that the present method is effective to improve the rate capability of the positive electrodes without lowering electrode density.

Keywords: Lithium battery; Rate capability; Carbon composite; Lithium nickel cobalt oxide; Spark-plasma-sintering

1. Introduction

For the electrode materials in practical lithium-ion batteries, particularly those in electric and hybrid-electric vehicles, higher rate capability together with higher energy density is one of the most important characteristics [1–3]. However, lithium-ion cells cycled at relatively high-current density or at elevated temperature exhibited a significant power loss, which is associated primarily with a rise of the cathode impedance [1,2,4–8]. For example, Itou and Ukyo reported a serious increase in resistance at $LiNi_{0.8}Co_{0.15}Al_{0.05}O_2$ (LNCA)-based positive electrodes when the cells were cycled at 60 °C under 2 C rate [4]. Although there exist several debates on the origin of the impedance rise, some of the diagnostic analyses on the LNCA-based electrodes indicated that a loss of the conductive carbon at the surface of the cathode particles, leading to the electrical disconnection between them, would be partly responsible for the impedance rise [5–8]. Therefore, a method to overcome this problem, for example, to make stronger binding among cathode particles and carbon additives, is required for high-power lithium-ion batteries.

Spark-plasma-sintering (SPS) is a process that makes use of microscopic electrical discharge between particles [9]. In this process, the powders loaded in the graphite die are pressed uniaxially (*ca.* 30–50 MPa), and a pulsed dc current (*ca.* 1000 A) is simultaneously applied to generate a spark discharge between particles, which generates an internal localized heating, promotes material transfer, accelerates the contacts between particles, and results in producing dense polycrystalline microstructures [9,10]. Recently, we have applied this method to $LiFePO_4$ and carbon powders as an attempt to form strong binding between them, and it was successful to prevent the electrical isolation of the active particles, which resulted in the improvement of the electrochemical performances [11]. For applying this technique to the oxide-based active materials such as LNCA, some modifications are required, because there is a serious problem of the reductive formation of Ni^{2+} under the SPS reductive conditions.

In the present work, we tried to improve the rate capability of the LNCA cathodes by forming strong bindings between active material and carbon powder, as well as those between carbon particles themselves. Our present methodology is schematically shown in Fig. 1. In order to form strong carbon–carbon contacts, we prepared high-density carbon powders HDAB by the conventional SPS-treatment of acetylene black (AB) powder using graphite-die. Such high-density carbon powders would assist to form well-developed electrical networks in the electrodes. To form active material–carbon contacts, we applied higher-pressure (*ca.* 500 MPa) SPS process using WC-die for

* Corresponding author.
E-mail address: takeuchi.tomonari@aist.go.jp (T. Takeuchi).

0378-7753/$ – see front matter © 2007 Elsevier B.V. All rights reserved.
doi:10.1016/j.jpowsour.2007.06.192

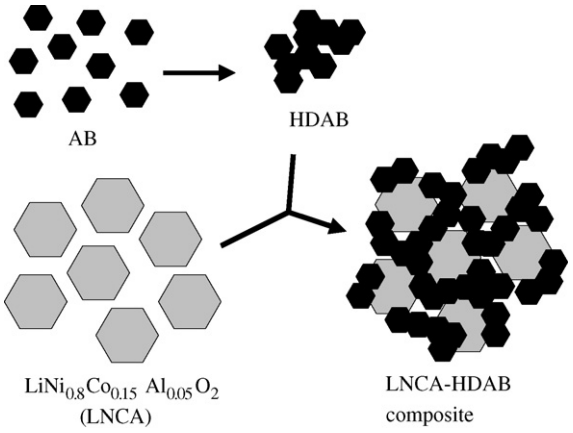

Fig. 1. Schematic representation of preparing HDAB powder and LNCA–HDAB composite sample.

the mixtures of LNCA and HDAB powders. WC-die would have an advantage of suppressing the reductive conditions during the SPS process as compared with the graphite-die, as well as an advantage of its higher applicable pressures. Using these techniques, we examined the factors to improve the electrochemical charge/discharge performances of the positive electrodes under higher current density.

2. Experimental

First, HDAB powder was prepared by the SPS treatment (SPS-515S, SPS Syntex Inc., Japan) of AB powder at 1000 °C for 1 min under the pressure of 30 MPa using graphite-die. The obtained HDAB was blended thoroughly with LNCA (Fuji Chemical Industry, Japan) in weight ratio of 1:9 and then allowed to the SPS treatment at 150–400 °C for 1 min under the pressure of 150–500 MPa using WC-die, to form the LNCA–HDAB composites. The blended sample of LNCA + HDAB was also used to examine the effect of binding between carbon particles.

The phase purity and cation distribution of the samples were checked by X-ray diffraction (XRD) measurement (Rotaflex RU-200B/RINT, Rigaku) using monochromatic Cu Kα radiation within the 2θ ranges of 10–125°. The RIETAN-2000 program was used for structural refinement with X-ray Rietveld analysis [12]. Morphology and elemental mapping of the samples were examined by scanning electron microscopy (SEM; Rigaku JSM-6390LA) and energy dispersive X-ray analysis (EDX; Rigaku JED-2300). The tap density was estimated from the sample weight and the volume in the measuring cylinder after tapping several tens times. The electrochemical lithium insertion/extraction reactions were carried out using lithium coin-type cells. The working electrode consisted of a mixture of a 22.2 mg LNCA–HDAB composite and a 0.5 mg Teflon powder pressed into a 15 mm diameter tablet under a pressure of 10 MPa. The electrochemical test cells were constructed in a stainless steel coin-type configuration. The negative electrode was a 15 mm diameter and 0.2 mm thick disk of Li foil or 50 μm thick MCMB sheet loaded on Cu foil (current collector), and the separator was a microporous polyolefin sheet. The solution of 1 M $LiPF_6$ in a 50:50 mixture of ethylene carbonate (EC) and diethylcarbonate (DEC) by volume (Tomiyama Pure Chemical Industries Ltd., battery grade) was used as the electrolyte. Cells were constructed in an argon-filled glove box, and the electrochemical measurements were carried out at 30 or 60 °C after standing overnight on open circuit using a TOSCAT-3100 (Toyo System) at current densities of 53 and 265 mA g^{-1} (0.2 and 1 C) between 4.2 and 2.75 V.

3. Results and discussion

The HDAB powder showed significantly higher tap density (0.18 g cm^{-3}) as compared with that (0.03 g cm^{-3}) of the original AB powder. However, the measured BET surface area remained almost unchanged (*ca.* 70 m^2 g^{-1}) irrespective of the SPS conditions. These results indicated that the HDAB powder consisted of similar-sized primary particles as those of the original AB powder, and its porosity was much reduced. SEM observations were consistent with these results; both HDAB and AB powders showed similar primary particles with the size of *ca.* 30–50 nm, while more open-spaces were observed in the AB powder than those of the HDAB. We also measured Raman spectra for both carbon powders in the range of 500–4000 cm^{-1} to examine the existence of impurities (such as organic residues and absorbed water) and the degree of graphite disorder, which is associated with the integrated peak intensity ratio of D- and G-bands (I_D/I_G) centered at 1360 and 1580 cm^{-1}, respectively [6–8]. The measured I_D/I_G values were almost identical for both powders (*ca.* 1.0), and any impurity peaks originated from organic functional groups were not observable. Therefore, almost no graphitization proceeded in the HDAB powder, and the effect of removing surface impurities during the SPS process [9,10] was not detected in the present analysis methods. XRD patterns also showed very similar profiles in both carbon powders, which is consistent with the results of Raman measurements.

The SPS-treated LNCA–HDAB composites were black in color, and their appearance was similar to that of the LNCA + AB conventionally blended powder. Each XRD peak of the composites was indexed by the hexagonal unit cell ($R\bar{3}m$), and the estimated lattice parameters (for example, $a = 2.86163(6)$ Å, $c = 14.1696(3)$ Å, for samples treated by SPS at 250 °C under 500 MPa) were in good agreement with those ($a = 2.86155(5)$ Å, $c = 14.1753(2)$ Å) before SPS treatment and previously reported values ($a = 2.862$ Å, $c = 14.171$ Å [13]). We also estimated the cation disordering by the occupancy of transition metal at $3a$ site using a layered rock-salt unit cell $[Li_{1-x}M_x]_{3a}[M]_{3b}O_2$ ($0 < x < 1$), because an increase in x value is associated with a capacity loss of the cells [14]. The x value of the LNCA–HDAB composites, estimated by the X-ray Rietveld analysis, was 0.010(1), which was very close to that ($x = 0.011(1)$) before SPS treatment, indicating that no cation disordering proceeded.

We firstly examined the effect of the applied pressure during the SPS process on the electrochemical performances. Fig. 2 shows the initial discharge curves of the LNCA–HDAB composite sample cells (using Li anode) at different current densities. The composite samples were prepared by the SPS treatment at 250 °C under the pressures of 150 and 500 MPa. The discharge

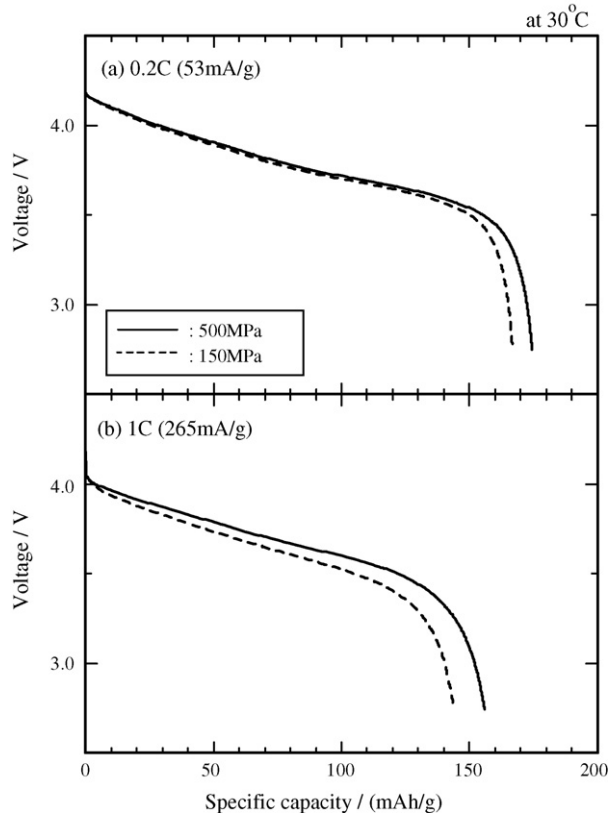

Fig. 2. Initial discharge profiles for LNCA–HDAB composite sample cells (using Li anode) at 53 and 265 mA g^{-1} (0.2 and 1 C). The composite samples were prepared by the SPS treatment at 250 °C under the pressures of 150 and 500 MPa.

capacity was enlarged and the averaged discharge voltage was elevated by applying higher pressure during the SPS process. This effect is more evident when the cells were cycled at higher current density. Since the structural parameters of the LNCA for these composite samples, estimated by the X-ray Rietveld analyses, were in good agreement with those of the original LNCA, higher applied pressure enhances the binding between the LNCA and carbon powders without affecting the reductive damage on the active material. This binding effect lowers the interparticle resistance among them, which resulted in higher discharge capacity and averaged voltage.

We also examined the effect of the SPS temperature on the electrochemical performances of the LNCA–HDAB composite sample cells. In this case, all the composite samples were prepared by the SPS treatment under 500 MPa. As shown in Fig. 3, the initial discharge capacity and the averaged discharge voltage showed some maximum values around 250 °C, and it is more evident when the cells were cycled at higher current density. In Fig. 3, interatomic distance of M_{3b}–O_{6c} (d_{M-O}) in LNCA and Li_2CO_3 content for the composite samples, estimated by the X-ray Rietveld analyses, are also plotted. d_{M-O}-value increased almost linearly with the rise of SPS temperature, and the Li_2CO_3 content showed significant increase above 300 °C. As in the decomposition mechanism of $LiNiO_2$ [14–16], the increase in d_{M-O} value suggests the formation of Ni^{2+}, because of the increase in ionic radii (Ni^{3+}(0.70 Å) < Ni^{2+}(0.83 Å) [17]). This would be associated with the elimination of Li^+, followed by the substitution of Ni^{3+} for vacant Li^+ site, leading to the change of valence state of Ni^{3+} to Ni^{2+} to maintain the electrical neutrality [14–16]. The eliminated Li would react with carbon and oxygen (and/or CO_2) to form Li_2CO_3 possibly on the surface of the active materials [16,18]. Therefore, the reduction and decomposition of LNCA during the SPS treatment might proceed according to the following reaction:

$$4LiNi_{0.8}Co_{0.15}Al_{0.05}O_2 + 2xC + 3xO_2 \rightarrow 4Li_{1-x}Ni_{0.8}Co_{0.15}Al_{0.05}O_2 + 2xLi_2CO_3.$$

Such reduction and decomposition became significant above 300 °C (Fig. 3), which resulted in the poor electrochemical performances of the cells. In contrast, the improvements of the discharge capacity and the averaged discharge voltage up to 250 °C would be originated from the formation of stronger binding between the LNCA and the carbon powders. Therefore, the present optimal SPS temperature, 250 °C, would be specified by balancing two conflicting factors of (i) the formation of the electrical connection between the active materials and the carbon powders and (ii) the reductive damage on the active materials. The latter factor, particularly the formation of Li_2CO_3 possibly on the surface of LNCA, seems critical in determining the electrochemical performances of the composite electrodes.

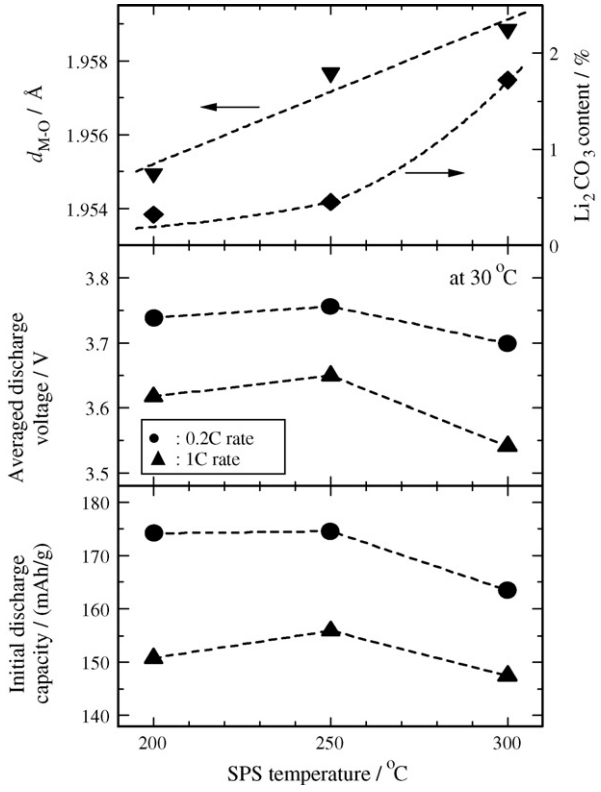

Fig. 3. Initial discharge capacity and averaged discharge voltage for LNCA–HDAB composite sample cells (using Li anode) at 53 and 265 mA g^{-1} (0.2 and 1 C) as a function of SPS temperature. Interatomic distance (M_{3b}–O) in LNCA and Li_2CO_3 content for the composite samples, estimated by the X-ray Rietveld analyses, are also plotted. All the composite samples were prepared by the SPS treatment under 500 MPa.

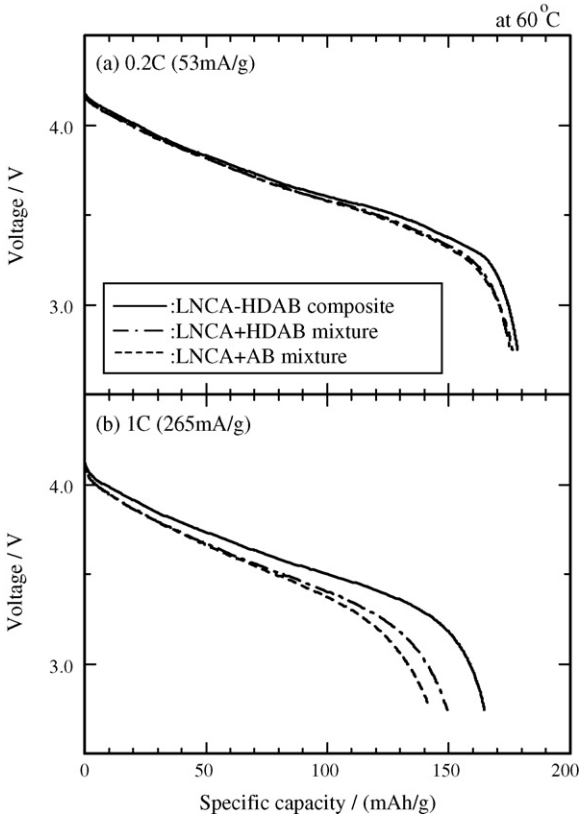

Fig. 4. Initial discharge profiles for LNCA + AB, LNCA + HDAB blended powders and LNCA–HDAB composite sample cells (using MCMB anode) at (a) 53 mAh g^{-1} (0.2 C) and (b) 265 mAh g^{-1} (1 C) measured at 60 °C.

The above improvement effect for the LNCA–HDAB composite sample was decomposed into two factors of interparticle electrical connections; (i) the carbon–carbon contact and (ii) the active material–carbon contact. The former factor was examined by comparing the electrochemical performances of the LNCA + AB and the LNCA + HDAB blended powder cells, and the latter factor by comparing those of the LNCA + HDAB blended powder and the LNCA–HDAB composite sample cells. Fig. 4 shows the initial discharge curves for the cells (using MCMB anode) with the above-mentioned three kinds of samples at different current densities. At 1 C rate, the discharge capacity was slightly enlarged by blending the HDAB, and further capacity enlargement, as well as higher averaged voltage, was achieved by forming the LNCA–HDAB composites. The former improvement is ascribed to the effect of the electrical carbon–carbon contact, and the latter to that of the active material–carbon contact, respectively. Judging from the discharge profiles in Fig. 4(b), the effect of the active material–carbon contact is a dominant factor to improve the electrochemical performances of the positive electrodes. These individual effects were not so evident when the cells were cycled at lower current density (Fig. 4(a)), though the cells with LNCA–HDAB composite samples showed slightly higher discharge capacity and averaged voltage as compared with those of other two samples. Such difference depending on the current density, as observed also in Figs. 2 and 3, indicate that the present composite effect is advantageous to improve the rate capability of the positive electrodes.

Table 1
Thickness (t (μm)), density (d (g cm^{-3})), and electrical conductivity (σ (S cm^{-1})) of the thin positive electrodes prepared from the LNCA + AB and LNCA + HDAB blended powders and the LNCA–HDAB composites

Sample	t (μm)	d (g cm^{-3})	σ (S cm^{-1})
LNCA + AB mixture	28	3.05	4.8×10^{-3}
LNCA + HDAB mixture	27	3.16	6.1×10^{-3}
LNCA–HDAB composite	27	3.21	5.0×10^{-3}

The present composite effect suggests that the electrical disconnection inside the positive electrodes, mainly between the LNCA and the carbon powders, is one of the key factors for the capacity fading of the cells cycled at higher current density. This is consistent with the previous reports that a loss of the conductive carbon at the surface of the cathode particles would be partly responsible for the impedance rise, resulting in the cell degradation [5–8].

As in our previous report [11], one of the advantages of the SPS-treated composite samples is the increase in the tap density. The tap density is a parameter showing how much the connections among the active materials and carbon powder are formed. The present LNCA–HDAB composite samples, treated by SPS at 250 °C under 500 MPa, also showed higher tap density (1.2 g cm^{-3}) as compared with that (1.0 g cm^{-3}) of the LNCA + HDAB and LNCA + AB blended powders. This would be advantageous for preparing higher density electrodes, leading possibly to manufacturing higher energy density battery cells. We actually prepared thin positive electrodes with the thickness of *ca.* 30 μm using the present LNCA–HDAB composite samples. The electrode thickness, its density, and electrical conductivity are listed in Table 1, together with those for the electrodes prepared from the LNCA + AB and

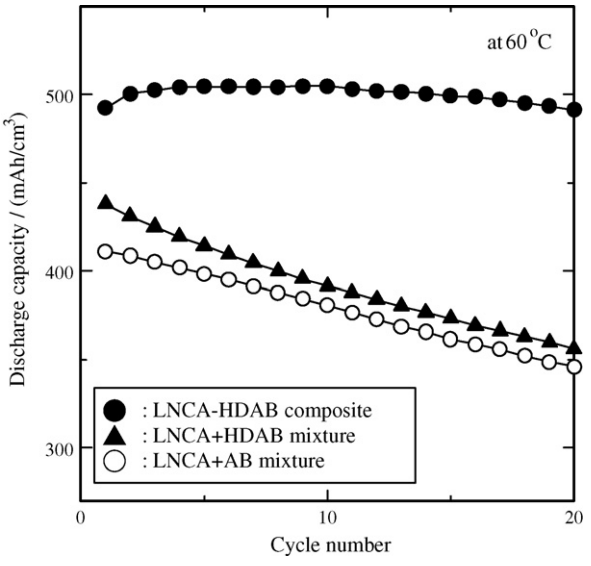

Fig. 5. Cycle performances for the thin positive electrode cells (using MCMB anode) prepared from LNCA + AB, LNCA + HDAB blended powders and LNCA–HDAB composite samples at 88 mA g^{-1} (1/3 C) measured at 60 °C.

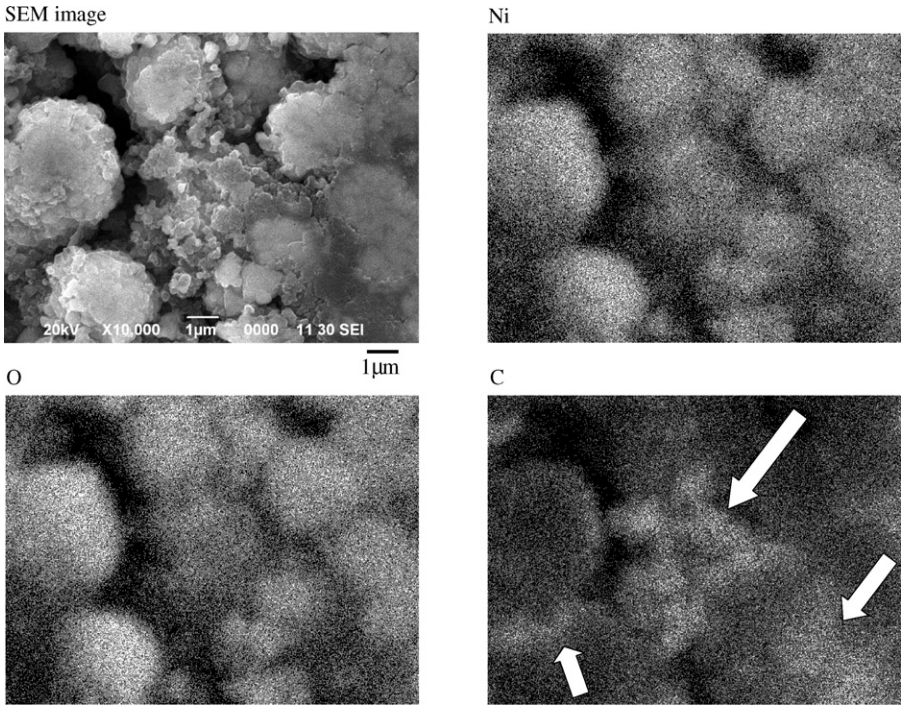

Fig. 6. SEM image and elemental mappings of Ni, O, and C atoms by EDX for the thin positive electrodes of LNCA–HDAB composite samples after electrochemical tests over 20 cycles at 88 mA g^{-1} (1/3 C). Magnification is the same for each photograph.

LNCA + HDAB blended powders for comparison. The electrode density increased by forming the LNCA–HDAB composites. This is consistent with the increase in the tap density for the LNCA–HDAB composite samples, as described above. A notable point is that the electrode density increased just by blending the HDAB, though both of the LNCA + AB and the LNCA + HDAB blended powders showed almost the same tap density values (1.0 g cm^{-3}). In addition, the change in the electrode density by blending the HDAB (*ca.* 3.6%, from 3.05 to 3.16 g cm^{-3}) was larger than that by the SPS treatment (*ca.* 1.6%, from 3.16 to 3.21 g cm^{-3}). These results suggest that the volumetric reduction of the carbon powders would mainly contribute to the increase in the electrode density. This would come from the bulky volume of carbon powders as compared with the compacted powders of the LNCA. The electrical conductivity of the electrode was nearly the same for these samples, and their effects seemed negligibly small.

Fig. 5 shows the cycle performances for the cells with the present three kinds of thin positive electrodes. The discharge capacity values were shown as those per electrode volume. By blending the HDAB powder, the discharge capacity enlarged, and by forming the LNCA–HDAB composites, further capacity enlargement was observed. Notably, the LNCA–HDAB composite cells showed much improved capacity retention (almost 100% after 20 cycles), as compared with those (81–84% retention) of other two sample cells. Thus, the present composite method is effective to improve the electrochemical performances without lowering the electrode density.

The present high capacity retention for the LNCA–HDAB composite sample cells suggests that the electrical connection remained almost unchanged during the electrochemical redox cycling. To examine the surface carbon coverage, we carried out the elemental mappings of Ni, O, and C for the LNCA–HDAB composite electrodes after electrochemical tests over 20 cycles. As shown in Fig. 6, the mapping profile of carbon atoms partly overlaps with those of nickel and oxygen; the carbon atoms were detected on the surface of the active materials and in their interparticle regions. Particularly, the presence of carbon atoms between the LNCA particles, as indicated by left-bottom and right-bottom arrows, indicates that the HDAB powder formed electrical bridges between the active materials. It is noteworthy that we often observed well-developed carbon networks which formed the agglomerates with the active materials; typical observation is indicated by a central arrow in Fig. 6. These results indicate that the carbon powder forms strong binding with the active materials in the composite samples, and they remained almost unchanged even after the electrochemical tests. This makes a clear contrast to the LNCA + HDAB blended electrodes, where the elemental mapping of carbon atoms rarely overlaps with those of the nickel and oxygen atoms. This result suggests the removal of carbon powder from the surface of active materials, which is consistent with the previous reports [5–8]. Thus, the formation of strong binding between the active materials and the carbon powders was one of the dominant factors to improve the electrochemical performances, and the present methodology to prepare the LNCA–HDAB composites by the SPS treatment under high pressure (*ca.* 500 MPa) was effective to achieve it.

4. Conclusion

We have successfully prepared dense LNCA–HDAB composite electrodes by the SPS treatment using the WC-die under

relatively high pressure (*ca.* 500 MPa). By blending the HDAB, the strong bindings between the carbon powders were formed, and by the SPS treatment, those between the active materials and carbon powders were formed. Both contact effects improved the electrochemical performances of the cells; particularly the electrical connections between the active materials and the carbon powders played a dominant effect for these improvements. These effects were more evident when the cells were cycled at higher current density, which indicates that the present method is effective to improve the rate capability of the positive electrodes without lowering the electrode density.

Acknowledgments

We thank Dr. Tatsuya Nakamura of Hyogo University for his stimulating discussion. This work was financially supported by R&D project for Li batteries by METI and NEDO.

References

[1] R. Kostecki, F. McLarnon, Electrochem. Solid State Lett. 5 (2002) A164.
[2] A.M. Andersson, D.P. Abraham, R. Haasch, S. MacLaren, J. Liu, K. Amine, J. Electrochem. Soc. 149 (2002) A1358.
[3] C.H. Chen, J. Liu, M.E. Stoll, G. Henriksen, D.R. Vissers, K. Amine, J. Power Sources 128 (2004) 278.
[4] Y. Itou, Y. Ukyo, J. Power Sources 146 (2005) 39.
[5] J. Shim, R. Kostecki, T. Richardson, X. Song, K.A. Striebel, J. Power Sources 112 (2002) 222.
[6] K.A. Striebel, J. Shim, E.J. Cairns, R. Kostecki, Y.-J. Lee, J. Reimer, T.J. Richardson, P.N. Ross, X. Song, G.V. Zhuang, J. Electrochem. Soc. 151 (2004) A857.
[7] R. Kostecki, F. McLarnon, Electrochem. Solid State Lett. 7 (2004) A380.
[8] J. Lei, F. McLarnon, R. Kostecki, J. Phys. Chem. B 109 (2005) 952.
[9] M. Tokita, J. Soc. Powder Technol. Jpn. 30 (1993) 790.
[10] Z. Shen, M. Nygren, J. Mater. Chem. 11 (2001) 204.
[11] T. Takeuchi, M. Tabuchi, A. Nakashima, T. Nakamura, Y. Miwa, H. Kageyama, K. Tatsumi, J. Power Sources 146 (2005) 575.
[12] F. Izumi, T. Ikeda, Mater. Sci. Forum 321–324 (2000) 198.
[13] I. Belharouak, W. Lu, D. Vissers, K. Amine, Electrochem. Commun. 8 (2006) 329.
[14] H. Arai, S. Okada, H. Ohtsuka, M. Ichimura, J. Yamaki, Solid State Ionics 80 (1995) 261.
[15] R. Kanno, H. Kubo, Y. Kawamoto, T. Kamiyama, F. Izumi, Y. Takeda, M. Takano, J. Solid State Chem. 110 (1994) 216.
[16] H.S. Liu, Z.R. Zhang, Z.L. Gong, Y. Yang, Electrochem. Solid State Lett. 7 (2004) A190.
[17] R. Shannon, Acta Crystallogr. A 32 (1976) 751.
[18] K. Matsumoto, R. Kuzuo, K. Takeya, A. Yamanaka, J. Power Sources 81/82 (1999) 558.